Iran. J. Ichthyol. (2025) 12(3): 248-265
P-ISSN: 2383-1561; E-ISSN: 2383-0964

ORIGINAL ARTICLE

Morphological responses of Common carp (*Cyprinus carpio*) to environmental stressors using geometric morphometric technique

Zohreh KHAMMAR[1], Fatemeh TABATABAEI YAZDI[*1], Saeed ZAHEDI[2]

[1]Department of Environment, Faculty of Natural Resources and Environment, Ferdowsi University of Mashhad, Mashhad, Iran.
[2]Department of Fisheries, Faculty of Natural Resources and Environment, Ferdowsi University of Mashhad, Mashhad, Iran.

Correspondence
f.tabatabaei@um.ac.ir

Article history:
Accepted 25 August 2025

Abstract

This study investigated the morphological and growth responses of juvenile common carp (*Cyprinus carpio*) to four environmental stressors: cadmium, malathion, pH, and moderate salinity. A total of 120 specimens were exposed to the treatments under controlled laboratory conditions. Standardized photographs were taken from the left lateral side, and 18 homologous landmarks were digitized using tpsDig software. Geometric morphometric analyses, including Procrustes superimposition, Principal Component Analysis (PCA), Canonical Variate Analysis (CVA), and Discriminant Function Analysis (DFA), were conducted using specify software. Results indicated significant differences in body shape among treatments, with cadmium exposure producing the most severe deformations in cranial and caudal regions and the greatest reduction in centroid size and standard length. pH caused notable shape changes in the ventral and anterior body regions. In contrast, salinity treatment led to increased centroid size and deeper body profiles, suggesting adaptive morphological plasticity. Malathion-exposed specimens showed mild but statistically significant changes, particularly in the abdominal and head areas. CVA and DFA confirmed high classification accuracy (81.33%) among treatments, demonstrating the sensitivity of geometric morphometrics in detecting stressor-induced shape variation. These findings highlight the utility of shape-based analyses as early indicators of environmental stress and support their application in freshwater biomonitoring programs.

Keywords: Geometric morphometric, Fish, Morphological plasticity, Heavy metals, Malathion

INTRODUCTION

Aquatic ecosystems are increasingly affected by multitude of anthropogenic stressors, including industrial effluents, agricultural runoff, and climate-induced changes. These factors alter the physicochemical properties of aquatic ecosystems, introducing stressors such as salinity fluctuations, pH shifts, heavy metal contamination (notably cadmium), and pesticide residues like malathion (van Emmerik et al. 2023; Bănăduc et al. 2024). Such environmental changes can significantly impact the morphological development and physiological homeostasis of fish, especially during their early life stages. Fish, being sensitive bioindicators, exhibit measurable morphological and biochemical responses to these stressors, making them ideal subjects for environmental monitoring (Valcarce et al. 2024; Ferizi et al. 2025).

Morphological plasticity is a well-documented adaptive response to environmental conditions among fishes (Mouludi-Saleh et al. 2022). In fishes, investigation of morphological variations showing morphological flexibility, regional adaptations, and changes in ecological characteristics (Seçer et al. 2020). Environmental conditions influence body shape, affecting swimming performance, energy allocation, feeding behavior, and survival. Traits such as body depth, head length, caudal peduncle width, and fin placement are highly variable and often reflect local environmental conditions (Shuai et al. 2018; Hansen et al. 2025). Analyzing shape variation thus offers insights into the ecological and developmental consequences of environmental stress (Ratunil et al. 2019; Alvarado-Flores et al., 2022).

Geometric morphometrics or GMM has emerged as a robust, statistically rigorous tool for quantifying

shape variation and visualizing morphological changes (Luo 2024). This method uses landmark-based data to retain geometric relationships between anatomical points, allowing researchers to detect subtle and localized shape differences (Vasconcelos et al. 2025). Recent studies have successfully applied GM to monitor fish exposed to specific environmental factors, such as pollution and temperature extremes (Adams & Otárola-Castillo 2013; Kelly et al. 2025).

Over the past decade, a growing body of research has explored the morphological impacts of environmental stressors on different fish species. For example, sub-lethal exposure to copper has been shown to significantly affect the morphological and functional development of fish embryos, including changes in body length and yolk sac area, as demonstrated in *zebrafish* (*Danio rerio*) (Johnson et al. 2007). Similarly, nutrient pollution has been linked to morphological and molecular alterations in Nile tilapia (*Oreochromis niloticus*), particularly in liver tissue, which reflects systemic stress responses (Behera et al. 2024). Exposure to pesticides has also been associated with distinct morphological and histological abnormalities in fish. A recent study reported structural damage in the gills, liver, and muscle tissues of freshwater fish following triazophos exposure, a commonly used *organophosphate pesticide* (Loganathan et al. 2024). Cadmium, even at low concentrations, has been shown to disrupt iron homeostasis and induce systemic inflammation in common carp (*Cyprinus carpio*), which can lead to both biochemical and morphological deviations (Guo et al. 2024). Furthermore, chronic exposure to heavy metals such as lead and mercury has been correlated with morphometric shifts and toxic accumulation in commercially important species like African catfish (*Clarias gariepinus*) and Nile tilapia, particularly affecting cranial and hepatic structures (Mavuti et al. 2021). These findings collectively underscore the value of morphometric analysis as a sensitive approach to detect ecological and developmental consequences of environmental stress.

Despite these valuable insights, several gaps remain unaddressed. Most existing studies have focused on adult or sub-adult fish, often under single-stressor conditions, which do not represent the complex nature of real aquatic environments. Furthermore, few studies have integrated morphological analysis with physiological metrics such as blood biochemistry, which may provide a more comprehensive view of organismal stress responses.

To fill this gap, the present study examines the combined effects of salinity, pH, cadmium, and malathion on the body shape and blood biochemical parameters of juvenile *Cyprinus carpio*, a commercially and ecologically important freshwater species. Using geometric morphometrics, we analyze landmark-based shape variation across treatments and integrate this with plasma biomarker measurements, including glucose, cortisol, total protein, cholesterol, and triglycerides.

This integrated approach allows us to capture both external morphological alterations and internal physiological stress responses in developing fish. To our knowledge, this is the first study to simultaneously assess the impact of multiple environmentally relevant stressors on juvenile carp using geometric morphometrics in combination with blood biochemistry. The findings aim to improve our understanding of early morphological indicators of stress, provide valuable data for aquaculture risk management, and contribute to bio-monitoring strategies in polluted freshwater systems.

MATERIALS AND METHODS

Studied species: The common carp (*Cyprinus carpio* Linnaeus, 1758) belong to Cyprinidae is one of the most widely cultured freshwater fish species in the world due to its high adaptability, fast growth rate, and economic importance (Page 2008). This species inhabits a variety of freshwater ecosystems including rivers, lakes, and ponds in Eurasia. Juvenile carp are highly sensitive to environmental stressors, making them an ideal model for studies on morphological variation and developmental plasticity (Tessema et al. 2020).

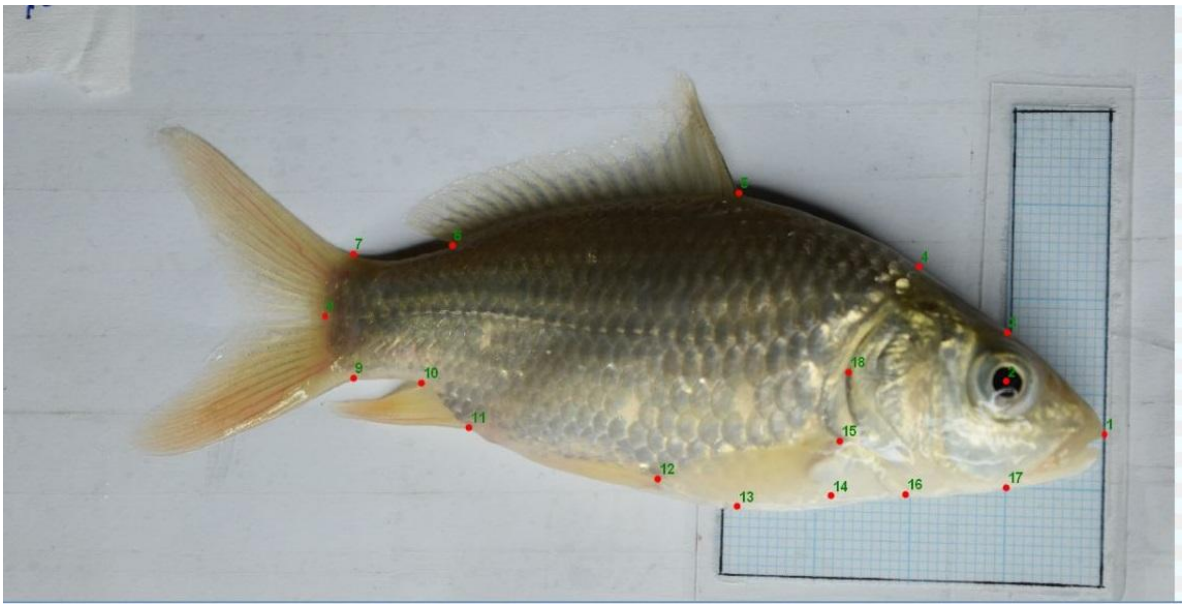

Fig.1. Annotated image showing the 18 landmarks on a juvenile common carp.

Table 1. Definition of anatomical landmarks.

Landmark Number	Definition
1	Tip of the snout at the upper jaw
2	Center of the eye
3	Intersection of the line marking the greatest head width at eye level
4	Upper margin of the operculum
5	Anterior base of the dorsal fin
6	Posterior base of the dorsal fin
7	Dorsal edge of the caudal peduncle
8	Posterior tip of the caudal peduncle
9	Ventral edge of the caudal peduncle
10	End of the anal fin base
11	Start of the anal fin base
12	Anterior base of the pelvic fin
13	Lowest point of the ventral body surface
14	Base of the pectoral fin (ventral point)
15	Base of the pectoral fin (dorsal point)
16	Posterior margin of the operculum
17	Lower edge of the operculum
18	Intersection of the line marking the lowest head width at eye level

In this study, a total of 150 specimens were nvestigated, 120 of which were used for treatment and 30 as controls.

Morphological Analysis: Morphological studies aim to assess body form deformations that arise due to environmental variations.

Geometric Morphometrics (GMM): GMM is a statistically powerful and visually interpretable tool that utilizes Cartesian coordinates of anatomical landmarks to analyze shape. Using this thechnique allowed us toinvestigate the sgave differences among the studied grous and to visualizethe deformations,without the confounding effects of size, position, or orientation (Klingenberg 2010).

Landmark types in morphometrics: In this study, 18 anatomical landmarks, including Type I and Type II (Webster et al. 2010), were digitized to capture variation in head structure, trunk depth, fin insertion, and caudal peduncle shape. The landmarks were selected based on established protocols for *Cyprinus carpio* (Zelditch et al. 2012) and are illustrated in Figure 1.

Landmark annotation: Landmarks were digitized using tpsDig2 software on standardized lateral images of juvenile common carp. Landmark positions were carefully selected to capture comprehensive morphological variation in fin insertion points, head structure, and body depth. The annotation process ensured repeatability and followed biological homology and geometric consistency standards (Mitteroecker & Gunz 2009).

Shape analysis: For landmark-based geometric morphometrics, specimens were aligned using the Generalized Least Squares (GLS) method (Rohlf & Slice 1990) to remove non-shape variation (i.e., size, position, orientation). For multivariate statistical shape analysis including PCA, CVA, and the generation of deformation grids and outlines, PAST software (version 4.17) and MorphoJ (version 1.08.02) (Klingenberg 2011) were used, respectively. Classification accuracy of the pre-groups were tested in PAST. Principal Component Analysis (PCA), Canonical Variate Analysis (CVA), and Discriminant Function Analysis (DFA) were performed inPAST and STATISTICA.Visualizations including deformation grids and outlines were created in MorphoJ. To quantify and visualize treatment-specific morphological variation, Discriminant Function Analysis (DFA) was employed. This multivariate technique maximizes separation between predefined groups (e.g., control vs. salinity-exposed fish) while minimizing within-group variance, making it ideal for detecting subtle but biologically meaningful shape differences (Zelditch et al. 2012). By transforming landmark coordinates into discriminant scores, DFA allows statistical evaluation of group distinctness and identification of anatomical regions contributing most to differentiation.

The pairwise groups comparisons and calculation of the statistical distances (Mahalanobis distances) between the studies groups' mean shapes. The pairwise comparisons in this study include the treatments and control group, as well.

Size analysis: Centroid size (CS) was calculated using PAST (version 4.17). To determine significant differences among groups, means and standard deviations were analyzed using Duncan's multiple range test in STATISTICA (version 14.0.0.15). Box plot graphs were generated in STATISTICAto visually represent size variation across the groups. The centroid size reflects the geometric size of the fish body shape configuration and is calculated as the square root of the sum of squared distances of all landmarks from the centroid. Standard length (SL) is a key indicator of somatic growth and developmental health in fish, and its analysis provides insight into how environmental stressors influence growth dynamics. In this study, in addition to CS, SL was also measured.

RESULTS

This section presents the results of geometric morphometric analyses conducted on juvenile common carp (*Cyprinus carpio*) exposed to different environmental stressors, including salinity, low pH, cadmium, and malathion. Using multivariate statistical tools such as Principal Component Analysis (PCA), Canonical Variate Analysis (CVA), and Discriminant Function Analysis (DFA), we evaluated patterns of body shape variation across treatment groups. In addition to shape differences, centroid size—a metric of overall body size—was assessed to determine how each treatment influenced somatic growth. The findings are illustrated through comparative statistics and visual representations such as scatterplots and deformation grids, providing a comprehensive view of morphological responses under stress conditions.

The box-whisker plot presented in Figure 2(a) illustrates the variation in centroid size—a key metric for overall body size in geometric morphometrics—among juvenile common carp (*Cyprinus carpio*) subjected to four different environmental stressors (salinity, malathion, cadmium, pH) and a control group. Among the treatment groups, fish exposed to salinity (S) exhibited the highest average centroid size, with the upper whisker extending close to 6200 units. This indicates that moderate salinity (6 ppt) may not inhibit and could potentially stimulate somatic growth or body elongation. However, the wide range and large standard deviation suggests significant inter-individual variability in response to salinity stress. In

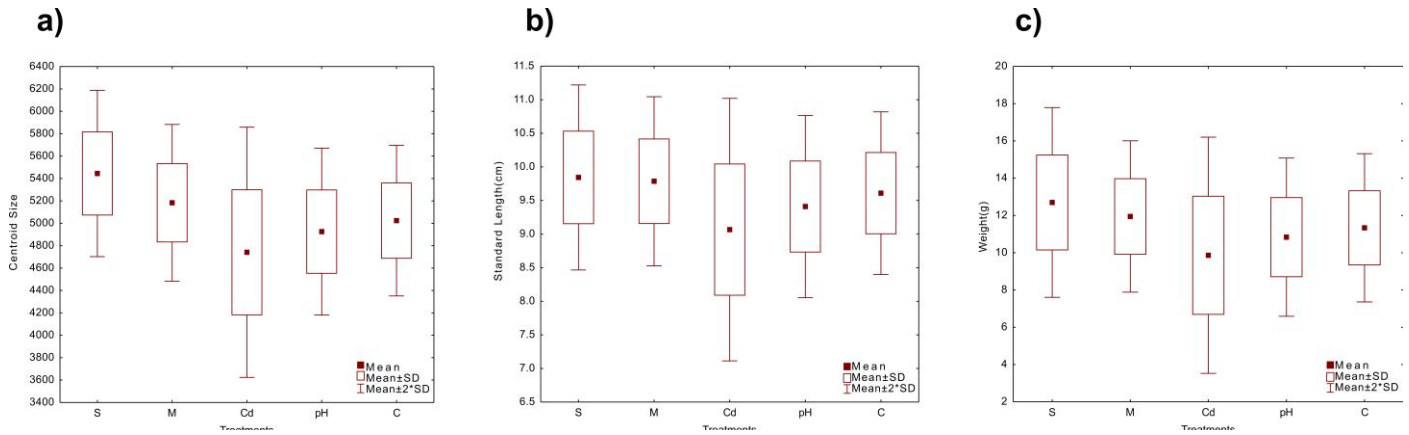

Fig.2. a) box plots showingsize differences among treatment groups. b) the variation in standard length among treatments groups (salinity, malathion, cadmium, and low pH) and control group. c) the distribution of body weight among juvenile *Cyprinus carpio* exposed to five experimental conditions: salinity (S), malathion (M), cadmium (Cd), low pH (pH), and control.

respect to malathion (M) treatment, the average centroid size was slightly lower than the salinity group but remained higher than cadmium, pH, and even the control group. The relatively narrower box and whiskers suggest a more uniform morphological response. Although malathion is known to disrupt physiological processes, in this study it did not severely reduce body size, possibly due to the relatively low concentration used. The most significant reduction in centroid size was observed in fish exposed to cadmium (Cd). This group exhibited the lowest mean centroid size, with values dropping to nearly 3600 at the lower end. The results suggest that cadmium exposure at 0.1 mg/L has a severe inhibitory effect on body growth, likely due to its interference with tissue development, ion regulation, and metabolic processes. The spread of data in this group was large, indicating varying levels of sensitivity among individuals. The pH (pH) group showed an intermediate centroid size—smaller than control, malathion, and salinity groups, but higher than cadmium. Exposure to acidic conditions (pH 5.5) likely induced moderate developmental stress, affecting body shape through altered osmoregulation and calcium metabolism. The control (C) group showed a median centroid size like the pH group but with less spread, which is expected under stable and non-stressed conditions. In summary, centroid size comparisons reveal that environmental stressors not only alter fish body shape but also significantly affect overall growth. Cadmium caused the most pronounced reduction in size, while salinity may have a growth-promoting or body-lengthening effect. These size-based results agree with shape-based analyses (e.g., PCA, CVA, DFA), highlighting the sensitivity of early developmental stages in *Cyprinus carpio* to pollutant exposure.

The box-whisker plot presented in Figure 2(b) shows the variation in standard length among *Cyprinus carpio* juveniles exposed to four environmental treatments (salinity, malathion, cadmium, and pH) and a control group. Among the treatment groups, fish exposed to salinity (S) demonstrated the highest mean standard length, (slightly above 10.0 units). This suggests that moderate salinity (6 ppt) did not hinder somatic growth and might even have exerted a stimulatory effect on body elongation, possibly through osmoregulatory adaptation. The relatively narrow distribution indicates a consistent growth pattern among individuals in this group. The malathion (M) group also exhibited a high mean standard length, comparable to that of the salinity group. Despite malathion being an organophosphate pesticide known to induce physiological stress, the low concentration used in this study (0.01 mg/L) may not have been sufficient to produce significant growth inhibition. The moderate spread suggests uniform developmental responses. In contrast, the cadmium (Cd) group showed the lowest mean standard length, with values extending as low as ~7.1 and high variability among individuals. This indicates that cadmium exposure

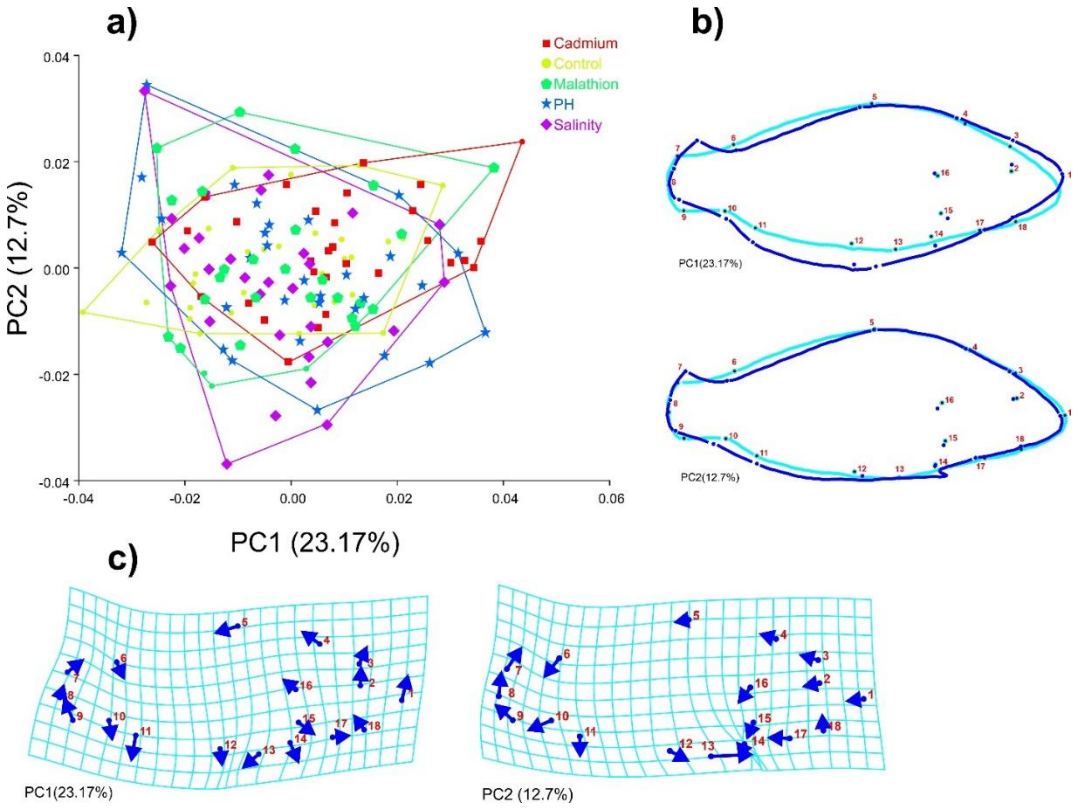

Fig.3. a) The PCA scatterplot. b) Outline shape variation along PC1 and PC2 in *Cyprinus carpio*. C) Deformation grids showing landmark shifts along PC1 (left) and PC2 (right).

(0.1 mg/L) had a strong inhibitory effect on growth, consistent with its well-documented toxicity and interference with metabolic and endocrine systems in fish. The wide range of values also implies variable sensitivity among individuals. Fish exposed to pH (5.5) had a mean standard length slightly lower than the control, suggesting moderate growth suppression likely due to acid-induced stress affecting ion regulation and bone development. The spread in this group was modest, indicating a more consistent but slightly diminished growth pattern. The control group (C) showed a stable mean standard length, slightly above 9.5, with low variability, representing expected growth under non-stress conditions. Overall, the analysis of standard length highlights clear growth suppression under cadmium and pH exposure, while salinity and malathion treatments had relatively minor effects. These findings are consistent with the centroid size results and suggest that growth-related traits are highly sensitive indicators of environmental stress in early-stage *Cyprinus carpio*.

The box-whisker plot in Figure 2(c) represents the distribution of body weight among juvenile *Cyprinus carpio* exposed to five experimental conditions: salinity (S), malathion (M), cadmium (Cd), pH (PH), and control (C). Body weight, as a fundamental indicator of growth and metabolic efficiency, reflects the integrated physiological status of fish under environmental stress. Among the groups, fish exposed to salinity (S) showed the highest mean body weight, exceeding 13 g, with some individuals approaching 18 g. This suggests that mild salinity (6 ppt) may enhance growth performance, possibly through improved osmoregulatory balance. However, the relatively wide interquartile range also indicates variability in the growth response, likely due to individual differences in adaptation. The malathion (M) group also exposed a relatively high mean weight, close to that of the salinity group, suggesting that at the applied concentration (0.01 mg/L), malathion did not significantly inhibit weight gain. The weight distribution in this group was more compact,

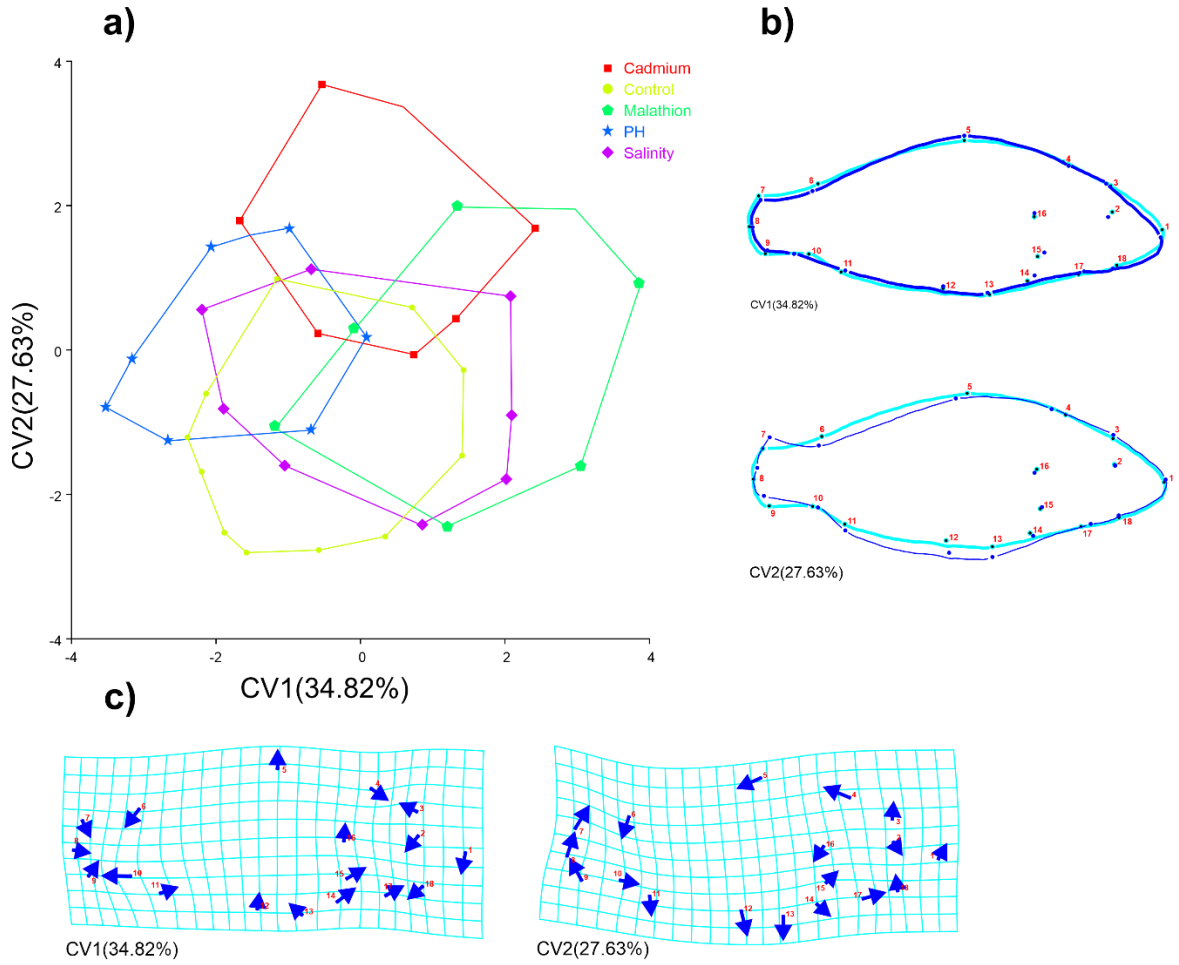

Fig.4. a) The CVA scatterplot. b) Outline shape variation along CV1 and CV2 in *Cyprinus carpio*. C) Deformation grids and outlines showing landmark shifts along CV1 (left) and CV2 (right).

indicating consistent physiological responses among individuals. In contrast, the cadmium (Cd) group had the lowest mean weight, with values ranging from approximately 3.5 to 16 g and a notably lower average (~9.5 g). This pattern reflects a substantial suppression of growth under cadmium exposure, in line with cadmium's known toxicity and disruption of metabolic, endocrine, and nutrient assimilation pathways. Species in the pH (pH) group exhibited moderate weight suppression, with average weights below those of salinity, malathion, and control groups. Acidic water can interfere with ionic balance and stress tolerance, leading to reduced feed efficiency and slower growth rates. The control (C) group maintained a stable mean weight (~11.5 g), serving as a reference for normal growth. The distribution was narrower than that observed in the cadmium or salinity groups, indicating healthy and consistent development in the absence of stress.

The PCA scatterplot of PC1 and PC2 in Figure 3 a) representing 23 and 13% of overlapping distributions among treatment groups. Fish exposed to cadmium and salinity displayed the greatest morphological dispersion, indicating higher variability and shape orientation under these stressors. In contrast, individuals from the control and pH groups were more centrally clustered, suggesting relatively stable body shape configurations. Malathion-treated fish showed moderate spread, reflecting subtle and heterogeneous shape changes. These findings confirm that environmental stressors induce treatment-specific morphological responses in *Cyprinus carpio*, particularly along shape dimensions associated with caudal peduncle, dorsal contour, and fin positioning.

Shape changes corresponding to the first two principal components are illustrated in Figure 3 (b) (outline overlays) and Figure 3. (c) (thin-plate spline deformation grids). PC1, which accounts for 23.17% of total shape variation. Notable displacements include inward movement of dorsal landmarks (5–9) and outward shift of ventral landmarks (11–14), indicating dorsoventral compression and expansion. Additionally, the caudal peduncle (landmark 17) shows lateral deformation, suggesting shape divergence in this region under stress conditions. PC2, explaining 12.7% of variation, represents changes focused around the cranial and abdominal areas. Landmarks associated with the snout and head (1–4) shift along the anterior-posterior axis, suggesting alterations in head length and orientation. Concurrently, ventral landmarks (12–15) exhibit downward and medial movement, indicating potential changes in abdominal fullness or curvature. These patterns highlight functionally distinct shape responses to environmental stressors, particularly in regions associated with locomotion and feeding.

The Canonical Variate Analysis (CVA) plot, presented in Fig.4 a) The CVA scatterplot. b) Outline shape variation along CV1 and CV2 in *Cyprinus carpio*. C) Deformation grids showing landmark shifts along CV1 (left) and CV2 (right). The illustrate group separation and shape deformation along the first two axes.

As shown in Figure 4 a) the scatterplot of CV1 (34.82%) and CV2 (27.63%) reveals distinction of treatment groups. The cadmium group (red) shows clear separation from other groups along the CV1 axis, indicating strong shape deformation. The control and pH groups overlap substantially, suggesting minimal morphological deformation under these conditions. Salinity and malathion treatments exhibit moderate spread, with partial overlap, reflecting intermediate effects on body shape. Figure 4 (b) outline comparisons between extreme values of CV1 and CV2 provide further visual evidence of localized morphological changes. CV1 deformations reflect dorsoventral compression and peduncular narrowing or widening. CV2 highlights variation in head slope and abdominal profile, supporting the notion that environmental stressors influence both axial and cranial body shape components. Figure 4 (c) displays thin-plate spline deformation grids for CV1 (right) and CV2 (left). Along CV1, major shifts are observed in landmarks on the dorsal (5–6) and ventral (12–14) surfaces, suggesting changes in body depth and caudal peduncle structure. CV2 emphasizes anterior-posterior displacements, particularly in cranial landmarks (1–4) and abdominal regions (15–17), indicating head shape modifications and ventral curvature variation under specific treatments

Pairwise comparisons of Mahalanobis distances (Table 2) revealed significant shape differentiation between treatment groups. The greatest distance was observed between the pH and malathion treatments, indicating substantial morphological divergence. Similarly, large distances were found between cadmium and pH, and cadmium and control (2.8592), reflecting the pronounced effects of cadmium on body shape. In contrast, the smallest distance observed between malathion and salinity (2.2339), suggesting more similar morphologies under these treatments. Procrustes distances, shown in Table 3, confirmed these patterns. The highest Procrustes value (0.0164) was recorded between salinity and cadmium, followed by malathion and cadmium (0.0162) and cadmium and control. Lower distances, such as those between salinity and control (0.0104) and malathion and salinity, indicate a lower degree of shape divergence in these pairs.

Classification accuracy from Canonical Variate Analysis (CVA) is summarized in Table 4. The overall correct classification rate was 81.33%, indicating strong discriminatory power of the shape-based model. The highest classification accuracy was found in the cadmium group (83.3%), followed closely by pH (90%) and control (90%). Misclassifications occurred primarily between malathion, salinity, and control, which is consistent with the smaller shape distances observed in Tables 2 and 3. These findings confirm the robustness of geometric morphometrics in detecting treatment-specific morphological responses in *Cyprinus carpio*.

Table 2. Pairwise Mahalanobis distances between treatment groups based on body shape variation in *Cyprinus carpio*. Higher values indicate greater morphological divergence.

	Cadmium	Control	Malathion	pH
Control	2.8592			
Malathion	2.7015	2.8282		
pH	2.9109	2.7854	3.1777	
Salinity	2.6897	2.4713	2.2339	2.5607

Table 3. Pairwise Mahalanobis distances between treatment groups based on body shape variation in *Cyprinus carpio*. Higher values indicate greater morphological divergence.

	Cadmium	Control	Malathion	pH
Control	0.0158			
Malathion	0.0162	0.0132		
PH	0.0140	0.0121	0.0152	
Salinity	0.0164	0.0104	0.0109	0.0139

Table 4. Classification results from Canonical Variate Analysis (CVA). (Overall accuracy: 81.33%).

	Salinity	Malathion	Cadmium	pH	Control	Total
Salinity	21	0	3	4	2	30
Malathion	2	22	3	2	1	30
Cadmium	1	1	25	1	2	30
pH	0	0	0	27	3	30
Control	0	2	0	1	27	30
Total	24	25	31	35	35	150

Discriminate analysis (DFA) was performed pairwise to assess the degree of morphological separation between treatment groups. The comparison between the control and salinity groups is illustrated in Figure 5. Figure 5 displays both the outline shape differences (left) and the histogram of discriminant scores (right) derived from DFA. Notable deformations are observed in the dorsal region (landmarks 4–6) and the caudal peduncle (landmarks 17–18), with salinity-treated fish exhibiting a more arched dorsal profile and a narrower posterior body. Subtle shifts in the ventral contour (landmarks 11–14) suggest compression or repositioning of the abdominal area under salinity stress. These shape differences indicate localized morphological plasticity, possibly linked to osmoregulatory adjustments in saline environments. The histogram of discriminant scores shows a clear separation between individuals from the control (red bars) and salinity (blue bars) groups. The minimal overlap between the distributions highlights the strong discriminatory power of the shape-based DFA model, confirming that salinity exposure induces consistent and statistically distinct morphological traits. Overall, the combination of landmark displacement patterns and group separation demonstrates the effectiveness of DFA in identifying treatment-specific shape variation. The observed deformation may reflect functional adaptations enhancing swimming efficiency or postural stability in response to salinity stress.

Discriminate function analysis between the control and pH treatment groups is shown on Figure 5 (b). The left panel displays outline-based shape differences, while the right panel presents the histogram of discriminant scores. The shape comparison reveals pronounced morphological deviations, particularly in the dorsal region (landmarks 4–6) and ventral mid-body (landmarks 12–14). Fish exposed to pH exhibited a more compressed dorsal profile and slightly deeper abdominal curvature compared to control individuals, suggesting adaptive changes in response to acidic stress, potentially affecting buoyancy and swimming efficiency. The histogram demonstrates clear group separation, with minimal

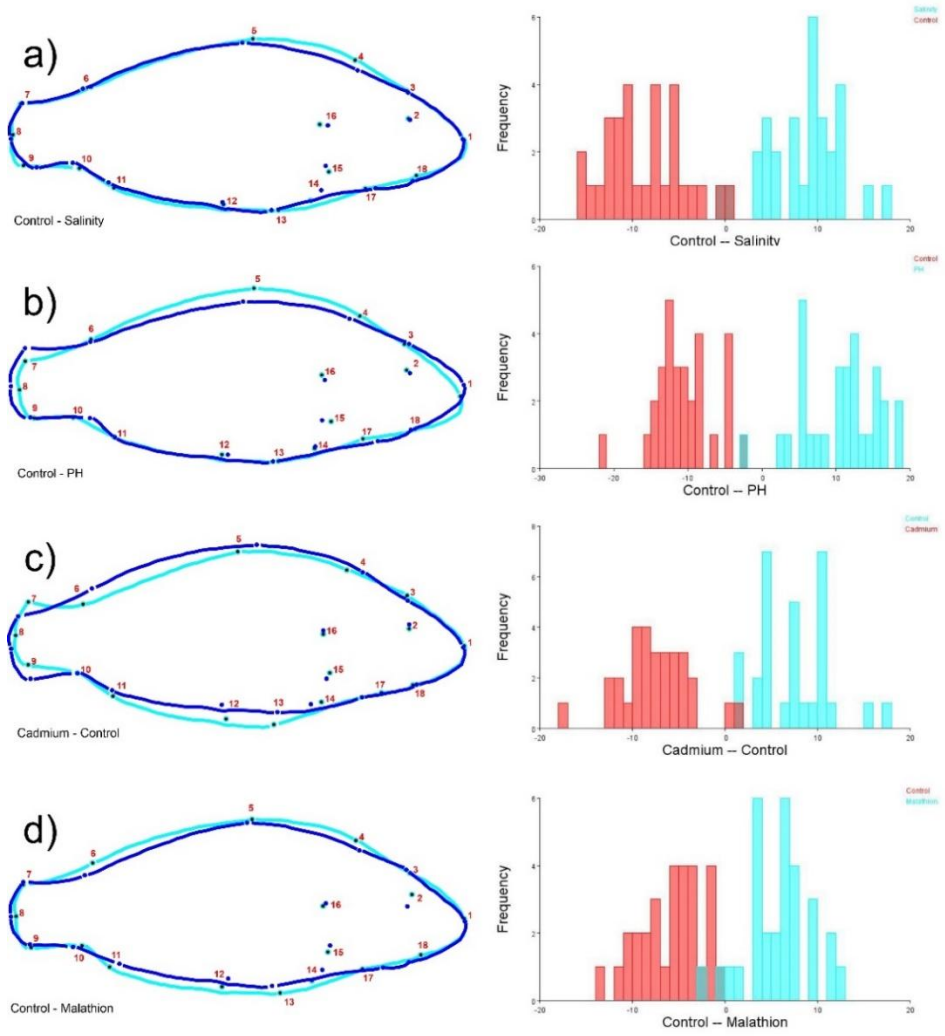

Fig.5. Shape differences (left) and discriminant scores (right): a) between control and salinity groups. b) between control and pH groups, c) between cadmium and control groups, and d) between control and malathion groups.

overlap between control (red) and pH (blue) groups. Most individuals cluster distinctly on opposite sides of the discriminant axis, indicating strong classification accuracy and confirming that acidic conditions result in measurable and consistent shape alterations. These findings underscore the capacity of DFA to distinguish shape-based responses to even moderate environmental changes such as pH reduction, validating the method's sensitivity in early developmental stages.

Discriminate function analysis comparing the cadmium and control groups is illustrated in Figure 5 (c). The left panel displays shape differences based on DFA outlines, and the right panel shows the distribution of individuals along the discriminant axis. Marked shape differences are observed across several regions of the body. Cadmium-exposed fish exhibit significant dorsal flattening (landmarks 4–6), along with contraction of the caudal peduncle and ventral region (landmarks 12–14, 17–18). In contrast, control fish maintain a more balanced and symmetrical body shape, reflecting normal developmental progression. These patterns suggest that cadmium exposure severely impacts body structure, likely through physiological stress, metabolic disruption, or impaired skeletal development. The histogram shows clear group separation, with cadmium (red) and control (blue) distributions occupying opposite ends of the discriminant function. Minimal overlap between groups confirms the high classification power of DFA and underscores the distinct morphological signature induced by cadmium exposure. This comparison

provides strong evidence that cadmium is the most morphologically disruptive stressor among those tested, as reflected in both landmark displacement and group clustering.

Discriminate function analysis comparing the control and malathion groups is illustrated in Figure 5 (d). The left panel depicts body shape differences based on DFA outlines, and the right panel shows the distribution of discriminant scores. The shape comparison reveals moderate yet consistent deformations. Fish exposed to malathion show subtle posterior elongation and a slightly more pronounced abdominal curvature (landmarks 12–14), whereas control fish maintain a more compact and symmetric shape. Notable changes are also visible in the cranial region (landmarks 2–3), indicating possible head displacement due to pesticide exposure. The histogram indicates clear, though less extreme, separation between the two groups. While some overlap exists, the majority of individuals cluster distinctly, supporting the idea that malathion induces mild but detectable morphological changes. These findings suggest that while malathion has a lesser impact on shape than cadmium or salinity, DFA remains effective in identifying subtle structural alterations linked to chemical exposure during early development.

Discriminate analysis comparing the pH and salinity groups is presented in Figure 6 (a). The left panel illustrates outline shape differences based on DFA, while the right panel shows the distribution of individuals along the discriminant axis. In the outline comparison, noticeable shape deviations are observed in the dorsal midline (landmarks 4–6), with pH-treated fish exhibiting a slightly flatter dorsal contour compared to the more arched dorsal profile seen in the salinity group. Additional differences are apparent in the ventral region, particularly around landmarks 12–14, where pH-exposed individuals show a slightly deeper abdominal curvature. These localized deformations suggest differential structural adaptation in response to acidic vs. saline environmental conditions. The histogram of discriminant scores shows a moderate but clear separation between the two groups. While there is some overlap between the red (pH) and blue (salinity) distributions, the majority of individuals cluster distinctly on either side of the discriminant axis. This supports the conclusion that shape-based DFA can reliably differentiate the morphological effects of pH and salinity exposure. Conclusively, the results highlight that although both stressors impact body shape, they do so through different anatomical pathways—pH affecting ventral curvature and salinity influencing dorsal and caudal form. These distinctions may reflect functional adaptations to acid stress versus osmoregulatory challenge.

Discriminate function analysis comparing cadmium and salinity groups is summarized in Figure 6 (b), with the left panel showing outline-based shape differences and the right panel displaying the histogram of discriminant scores. The shape comparison reveals pronounced morphological deviations, particularly in the ventral contour (landmarks 11–14) and dorsal region (landmarks 4–6). Cadmium-treated fish display a flatter ventral profile and slightly retracted head region, while salinity-exposed individuals exhibit a more pronounced dorsal arch and deeper body. These shape shifts reflect stress-specific developmental alterations, potentially tied to heavy metal toxicity versus osmoregulatory adaptation. The histogram on the right shows strong group separation, with minimal overlap between the cadmium (red) and salinity (blue) distributions. This clear distinction indicates high discriminatory power of the DFA model and supports the effectiveness of geometric morphometrics in differentiating stressor-specific effects on fish morphology. Overall, the comparison underscores that cadmium and salinity elicit distinct morphological responses, which can be reliably captured using landmark-based shape analysis.

Discriminate analysis between the malathion and salinity treatment groups is illustrated in Figure 6 (c). The left panel shows outline-based shape differences, while the right panel presents the histogram of discriminant scores derived from DFA. The outline comparison reveals moderate shape changes between

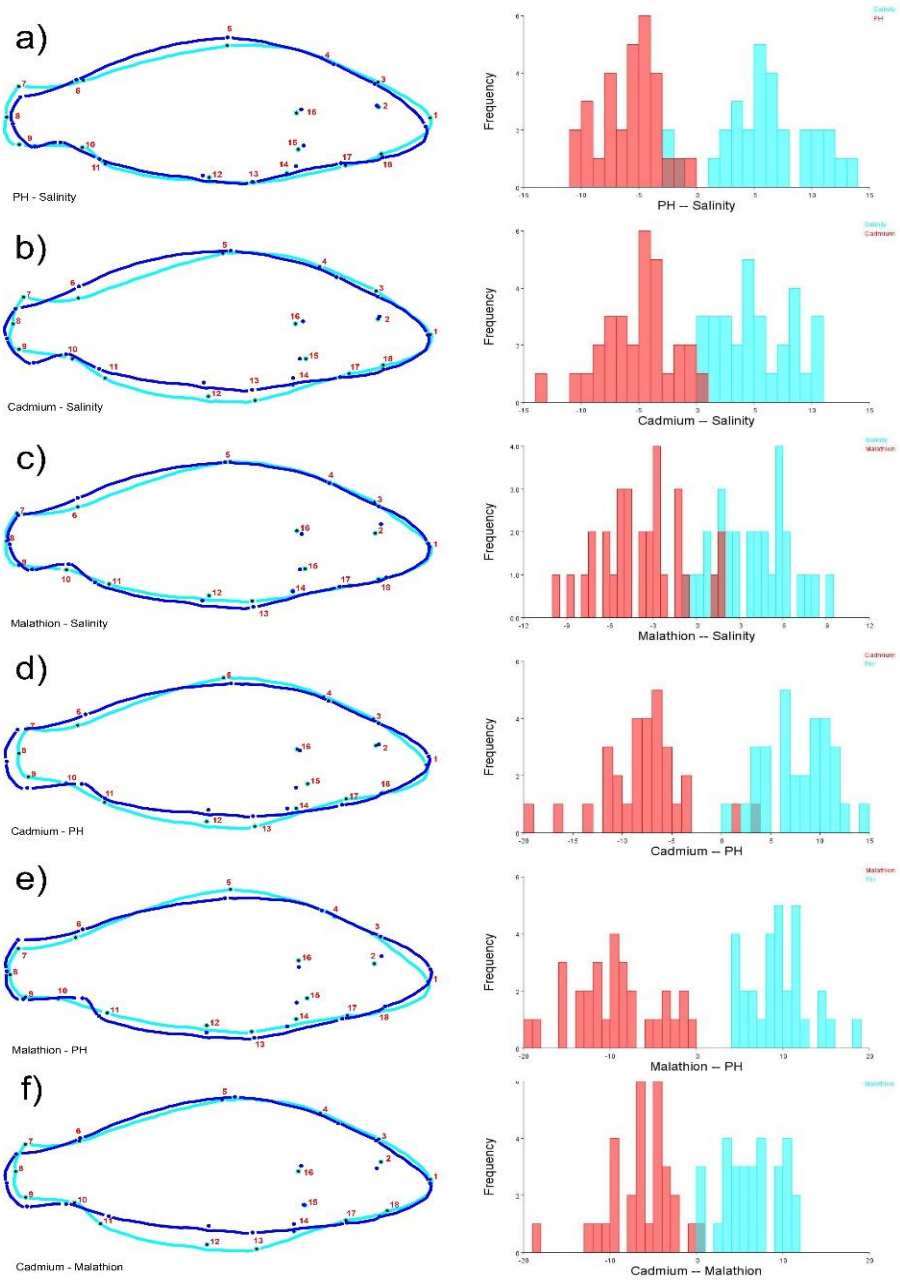

Fig.6. a) DFA-based comparison between pH and salinity groups. Left: shape differences showing dorsal and ventral contour shifts. Right: histogram of discriminant scores with partial group separation. b) DFA-based comparison between cadmium and salinity groups. Left: shape differences highlighting dorsal and ventral shifts. Right: histogram showing clear group separation. c) DFA-based comparison between malathion and salinity groups. Left: shape differences in head and abdominal regions. Right: histogram showing partial group separation. d) DFA comparison between cadmium and pH groups. Left: shape differences in head, dorsal, and ventral regions. Right: histogram showing clear group separation. e) DFA comparison between malathion and pH groups. Left: outline shape differences. Right: histogram showing distinct group separation. f) DFA comparison between cadmium and malathion groups. Left: shape deformation in head and trunk regions. Right: Histogram showing strong morphological separation.

the two groups. Key differences are seen in the head region (landmarks 2–4) and ventral contour (landmarks 12–14). Fish exposed to salinity exhibit a more arched dorsal profile and deeper abdominal curvature, while those in the malathion group show a flatter body shape, particularly in the cranial and mid-body zones. These differences may reflect altered muscle tone or developmental plasticity in response to chemical vs. osmotic stress. The discriminant score histogram shows partial but clear separation between

the two groups. Although some overlap exists, most individuals from each group cluster on opposite sides of the axis, indicating a moderate level of classification accuracy. This supports the presence of treatment-specific morphological traits distinguishable by DFA, though less pronounced than in cadmium comparisons. Overall, the results indicate that malathion and salinity induce distinguishable but less extreme shape differences and highlight the capacity of morphometric tools to detect subtle structural changes.

Discriminate analysis between the cadmium and pH treatment groups is presented in Figure 6 (d). The left panel illustrates shape differences based on DFA outlines, while the right panel shows the distribution of discriminant scores for both groups. In the shape comparison, distinct deformations are observed, particularly in the head region (landmarks 2–4), dorsal contour (landmark 5), and ventral midsection (landmarks 12–14). Fish exposed to cadmium display a more compressed body with posterior displacement of landmarks, whereas those under pH show a rounder ventral profile and slightly elevated head contour. These differences indicate stress-or-specific impacts on skeletal development and body configuration. The histogram shows a clear separation between cadmium (red) and pH (blue) groups, with minimal overlap. The distributions are well-separated along the discriminant axis, demonstrating high classification accuracy and confirming that the two stressors induce distinct morphological signatures. Overall, these findings highlight the capacity of DFA to differentiate between the effects of heavy metal toxicity and acid stress on body shape, even when both exert significant developmental pressure.

Discriminant analysis comparing the malathion and pH treatment groups is presented in Figure 6 (e). The left panel illustrates outline-based shape differences, while the right panel shows the frequency distribution of discriminant scores. Shape deformations between the two groups are most evident in the dorsal contour (landmarks 4–6) and head region (landmarks 2–3), with fish exposed to pH displaying a slightly more elevated dorsal profile and cranial prominence. Meanwhile, malathion-exposed fish tend to exhibit a flatter body and retracted head. Subtle differences are also noted in the ventral midline (landmarks 12–14), indicating changes in abdominal contour. The histogram reveals a clear and consistent group separation, with malathion (red) and pH (blue) groups occupying opposite ends of the discriminant axis. The lack of significant overlaps highlights the discriminative power of the model and confirms that the two chemical stressors elicit distinct and quantifiable morphological responses. These results underscore the ability of DFA to resolve fine-scale shape differences caused by different environmental pollutants, even when both have systemic effects on early development.

Discriminate function analysis between the cadmium and malathion treatment groups is shown in Figure 6 (f). The left panel illustrates shape differences based on outline deformation, while the right panel presents the discriminant score distribution histogram. The shape comparison reveals extensive morphological deviations between the two groups. Cadmium-exposed fish display a significantly more compressed body, especially along the ventral profile (landmarks 11–14) and dorsal surface (landmarks 4–6), while malathion-treated fish maintain a more balanced body contour. Additionally, anterior landmarks (2–3) show forward displacement in the cadmium group, suggesting possible head retraction due to developmental stress. The histogram highlights strong group separation, with cadmium (red) and malathion (blue) individuals clustering on opposite sides of the discriminant axis. The minimal overlap indicates high classification accuracy, confirming that the two treatments result in clearly distinguishable morphological outcomes. These results emphasize that cadmium, as a heavy metal, has a more disruptive effect on fish body shape than the pesticide malathion, with clear anatomical markers detectable through geometric morphometrics.

Statistical analysis results with *P*-values

Centroid size analysis: The analysis revealed a statistically significant difference in centroid size among the treatment groups ($P<0.001$). Notably, the

salinity treatment exhibited a larger centroid size compared to the other treatments, indicating a pronounced effect of salinity on overall body size.

Body length and weight analysis: Significant differences in body length and weight were observed between the experimental groups (P<0.001). Among all treatments, the cadmium-exposed group displayed the lowest mean body length, although considerable overlap in body size was evident among the remaining groups.

Principal Component Analysis (PCA): PCA results identified three principal components as statistically significant, collectively accounting for 47.12% of the total shape variance. The first principal component captured the most substantial variation in body morphology.

Canonical Variate Analysis (CVA): VA extracted two statistically significant canonical variables, which together explained 62.45% of the total variation. These axes highlighted distinct morphological differentiation among treatment groups, particularly in relation to specific anatomical landmarks.

DISCUSSION

This study assessed the morphological and growth responses of juvenile *Cyprinus carpio* under exposure to four stressors: salinity, pH, cadmium, and malathion. Using geometric morphometric techniques, significant body shape variations were detected among treatment groups, with cadmium eliciting the most pronounced deformations, particularly in the cranial and ventral regions. These results confirm the sensitivity of juvenile carp to even moderate environmental disturbances. The centroid size analysis revealed statistically significant differences across all treatments (P<0.001), indicating that environmental stressors not only impact shape but also overall somatic growth. Among the treatments, salinity-exposed fish exhibited the highest centroid size, suggesting that moderate salinity (6 ppt) may enhance growth, possibly via improved osmoregulatory balance. Conversely, cadmium exposure caused the most severe reduction in centroid size, consistent with its known inhibitory effects on tissue development and metabolic function. Likewise, body length and weight showed statistically significant reductions in certain groups (P<0.001). Fish in the cadmium treatment exhibited the shortest average body length and lowest mean weight, highlighting cadmium's suppressive impact on somatic development. In contrast, salinity and malathion treatments maintained or even promoted growth, suggesting a less detrimental or possibly adaptive physiological response under those conditions.

Our investigation on shape differentiation (PCA) confirmed that shape changes were driven primarily by variations in dorsal-ventral contour, cranial structure, and caudal peduncle morphology. Discriminate Function Analysis (DFA) demonstrated strong classification accuracy, with an overall correct classification rate of 81.33%. Notably, the cadmium and pH groups were most accurately classified, reflecting their distinctive morphological signatures.

The integration of shape metrics with growth parameters provides compelling evidence for stress-or-specific responses. For example, cadmium-induced shape deformations were associated with both cranial retraction and ventral flattening, while salinity led to deeper body profiles and expanded dorsal curvature. Malathion, although less disruptive, still produced detectable shape changes, particularly in the cranial and abdominal regions.

The morphological responses observed in this study align with and expand upon findings from earlier research on environmental stress in fish. For instance, the severe body deformations and reduced centroid size under cadmium exposure are consistent with studies on Cyprinus carpio by Guo et al. (2024), who reported cadmium-induced hepatic ferroptosis and systemic inflammation leading to growth suppression. Similarly, the dorsal flattening and caudal peduncle narrowing in our cadmium-treated group mirror the morphological disruptions documented in zebrafish (*Danio rerio*) exposed to copper (Johnson et al. 2007), suggesting conserved toxicological pathways across teleost. In contrast, our observation of enhanced centroid size and deeper

body profiles under salinity diverges from some studies on freshwater species but parallels work on euryhaline fish. For example, Bonzi (2022) noted similar adaptive plasticity in Oreochromis niloticus, where moderate salinity improved osmoregulatory efficiency and growth. This suggests that C. carpio may retain a partial euryhaline capacity, a trait less emphasized in prior literature. The mild but significant shape changes induced by malathion corroborate findings by Ullah et al. (2025), who identified sublethal pesticide effects on cranial and abdominal morphology in Labeo rohita. However, our study detected less severe impacts, possibly due to lower exposure concentrations or species-specific tolerance. Notably, the PCA and DFA results (81.33% classification accuracy) resonate with geometric morphometric applications in other stress studies, such as Vasconcelos et al. (2025), who successfully discriminated fish stocks using landmark-based methods. Yet, our integration of multiple stressors (unlike single-stressor designs in Alvarado-Flores et al. 2022) provides a more ecologically relevant perspective on cumulative effects.

While most studies (e.g., Bănăduc et al. 2024) focus on isolated stressors, our work demonstrates how concurrent exposure to salinity, pH, and pollutants elicits distinct morphological signatures. Also, prior research often examines adults (e.g., Hansen et al. 2025), but our focus on juveniles reveals heightened sensitivity during critical developmental windows. These comparisons underscore the novelty of our approach while contextualizing results within established toxicological and morphometric frameworks. These findings emphasize the utility of geometric morphometrics in capturing subtle morphological deviations and reinforce its application in early stress detection and ecological risk assessment. Furthermore, the inclusion of statistical significance values (p-values) strengthens the interpretation of morphological differences and supports their biological relevance. Ultimately, the study contributes valuable insights into how multiple environmental stressors influence the phenotypic plasticity of an economically important species, underlining the need for integrated biomonitoring frameworks in freshwater ecosystems.

CONCLUSION

This study demonstrated the high morphological sensitivity of juvenile *Cyprinus carpio* to a range of the studied stressors—specifically cadmium, malathion, pH, and elevated salinity—using landmark based geometric morphometric method. Cadmium emerged as the most adverse agent, inducing significant deformations in cranial and caudal regions and causing marked reductions in centroid size and standard length ($P<0.001$). pH exposure also resulted in distinct shape alterations, particularly in the ventral curvature and anterior profile, potentially reflecting acid-induced disturbances in osmoregulatory processes and skeletal development. In contrast, moderate salinity exposure led to increased centroid size and deeper body profiles, which may indicate adaptive morphological plasticity aimed at optimizing physiological function under brackish conditions (Bonzi 2022). Malathion exposure produced significant shape changes—mainly in the cranial and abdominal regions, suggesting mild sub-lethal effects on tissue development. Geometric morphometric technique effectively captured treatment-specific shape variations. classification accuracy 81.33%, with the highest group separation observed in cadmium and pH treatments were supported by significant *P*-values, confirming the biological relevance of the observed morphological responses. The study highlights the value of shape-based morphometrics as early-warning tools for detecting environmental stress, providing a cost-effective and visually interpretable alternative to more invasive biomonitoring techniques. However, certain limitations must be acknowledged. The study focused on early juveniles and acute exposures, which may not reflect long-term effects or recovery potential. Additionally, the absence of physiological and molecular data limits understanding of the underlying mechanisms driving shape changes. Future research should assess the persistence, reversibility, or developmental compensation of these shape changes over longer timeframes and across different life

stages. Expanding taxonomic diversity and integrating physiological data will further enhance the ecological validity and practical applicability of geometric morphometrics in freshwater toxicology and environmental monitoring.

REFERENCES

Adams, D.C. & Otárola-Castillo, E. 2013. geomorph: an R package for the collection and analysis of geometric morphometric shape data. Methods in Ecology and Evolution 4(4): 393-399.

Alvarado-Flores, J.; Arzate-Cárdenas, M.A.; Pérez-Yañez, D. & Cejudo, E. 2022. Environmental stressor induces morphological alterations in *zooplankton*. Latin American Journal of Aquatic Research 50(1): 1-12.

Bănăduc, D.; Curtean-Bănăduc, A.; Barinova, S.; Lozano, V.L.; Afanasyev, S.; Leite, T. & Cianfanglione, K. 2024. Multi-interacting natural and anthropogenic stressors on freshwater ecosystems: their current status and future prospects for 21st century. Water 16(11): 1483.

Behera, B.K.; Nayak, C.; Rout, A.K.; Pradhan, S.P.; Parida, P.K.; Sarkar, D.J. ... & Rai, A. 2024. Transcriptome profiling of Nile tilapia (*Oreochromis niloticus*) identifies candidate genes in response to riverine pollution. Current Research in Biotechnology 7: 100180.

Bonzi, L.C. 2022. Molecular Mechanisms Underlying Fish Phenotypic Plasticity in the Acclimation to Environmental Stressors.

Ferizi, R.; Ramadan, M.F.; Karataş, A. & Maxhuni, Q. 2025. Physiological and biochemical parameters in two fish species (*Scardinius erythrophthalmus* and *Cyprinus carpio*) in different rivers of Kosovo. Journal of Wildlife and Biodiversity 9(1): 200-219.

Guo, W.; Zhang, J.; Zhang, X.; Ren, Q.; Zheng, G.; Zhang, J. & Nie, G. 2024. Environmental cadmium exposure perturbs systemic iron homeostasis via hemolysis and inflammation, leading to hepatic ferroptosis in common carp (*Cyprinus carpio* L.). Ecotoxicology and Environmental Safety 275: 116246.

Hansen, M.J.; Muir, A.M.; Bronte, C.R. & Krueger, C.C. 2025. Phenotypic variation among four Lake Trout morphs at six locations in Lake Superior. Transactions of the American Fisheries Society 154(1): 68-84.

Johnson, A.; Carew, E. & Sloman, K.A. 2007. The effects of copper on the morphological and functional development of *zebrafish embryos*. Aquatic Toxicology 84(4): 431-438.

Kelly, M.; Barão, K.R. & Jacobina, U.P. 2025. Geometric morphometrics in fish studies: trends and scientific impacts—a scientometric and systematic mapping. Zoomorphology 144(2): 1-15.

Klingenberg, C.P. 2010. Evolution and development of shape: integrating quantitative approaches. Nature Reviews Genetics 11(9): 623-635.

Loganathan, K.; Tennyson, S. & Arivoli, S. 2024. Triazophos toxicity induced histological abnormalities in *Heteropneustes fossilis* Bloch 1794 (*Siluriformes: Heteropneustidae*) organs and assessment of recovery response. The Journal of Basic and Applied Zoology 85(1): 1-25.

Luo, D. 2024. Quantitative Analysis of Fish Morphology Through Landmark and Outline-based Geometric Morphometrics with Free Software. Bio-protocol 14(20): e5087.

Mavuti, S.K.; Mbaria, J.M.; Maina, J.G.; Mbuthia, P.G. & Waruiru, R.M. 2021. Levels of lead, mercury and cadmium in farmed *Oreochromis niloticus* and *Clarias gariepinus* in Nyeri County, Kenya. International Journal of Fisheries and Aquatic Studies 9(4): 230-233.

Mitteroecker, P. & Gunz, P. 2009. Advances in geometric morphometrics. Evolutionary Biology 36: 235-247.

Mouludi-Saleh, A.; Eagderi, S.; Abbasi, K. & Nasri, M. 2022. Validation of two sympatric fish species of Urmia chub, *Petroleuciscus ulanus* and Urmia bleak, *Alburnus atropatenae*, based on morphologic characters in Mahabad-Chai River. Nova Biologica Reperta 8(4): 289-296.

Page, L.M. 2008. Handbook of European freshwater fishes. Copeia 2008(3): 725-727.

Ratunil, V.B.; Libay, C.P.; Borja, E.A.; Ebarsabal, G.A.; Gamboa, G.Z.; Mahomoc, D.Q. ... & Cabuga, C. C. 2019. Analysis of body shape variation in *Glossogobius giuris* (Hamilton 1882) sampled from Lake Mainit, Philippines, using geometric morphometrics. International Journal of Fisheries and Aquatic Studies 7(2): 287-294.

Seçer, B.; Mouludi-Saleh, A.; Eagderi, S.; Çiçek, E. & Sungur, S. 2020. Morphological flexibility of *Oxynoemacheilus seyhanensis* in different habitats of Turkish inland waters: A case of error in describing a populations as distinct species. Iranian Journal of Ichthyology 7(3): 258-264.

Shuai, F.; Yu, S.; Lek, S. & Li, X. 2018. Habitat effects on intra-species variation in functional morphology: Evidence from freshwater fish. Ecology and Evolution 8(22): 10902-10913.

Tessema, A.; Getahun, A.; Mengistou, S.; Fetahi, T. & Dejen, E. 2020. Reproductive biology of common carp (*Cyprinus carpio* Linnaeus, 1758) in Lake Hayq, Ethiopia. Fisheries and Aquatic Sciences 23: 1-10.

Ullah, S.; Ahmad, S.; Ashraf, M.K.; Bilal, M.; Iqbal, T. & Azzam, M.M. 2025. Exposure to Acute Concentration of Malathion Induced Behavioral, Hematological, and Biochemical Toxicities in the Brain of *Labeo rohita*. Life 15(2): 158.

Valcarce, D.G.; Sellés-Egea, A.; Riesco, M.F.; De Garnica, M.G.; Martínez-Fernández, B.; Herráez, M.P. & Robles, V. 2024. Early stress exposure on zebrafish development: Effects on survival, malformations and molecular alterations. Fish Physiology and Biochemistry 50(4): 1545-1562.

van Emmerik, T.H.; Kirschke, S.; Schreyers, L.J.; Nath, S.; Schmidt, C. & Wendt-Potthoff, K. 2023. Estimating plastic pollution in rivers through harmonized monitoring strategies. Marine Pollution Bulletin 196: 115503.

Vasconcelos, J.; Cirera, M.; Vieira, A.R.; Otero-Ferrer, J.L. & Tuset, V.M. 2025. Application of shape analysis for the identification of pelagic fish stocks. Hydrobiologia 852(11): 2847-2869.

Webster, M.A.R.K. & Sheets, H.D. 2010. A practical introduction to landmark-based geometric morphometrics. The Paleontological Society Papers 16: 163-188.

Zelditch, M.; Swiderski, D. & Sheets, H.D. 2012. *Geometric morphometrics for biologists: a primer*. academic press.

Iran. J. Ichthyol. (2025) 12(3): 248-265
P-ISSN: 2383-1561; E-ISSN: 2383-0964
http://www.ijichthyol.org

doi: 10.22034/iji.v12i3.1019

مقاله کامل

پاسخ‌های ریختی ماهی کپور معمولی (*Cyprinus carpio*) به استرس‌های محیطی با استفاده از روش ریخت‌سنجی هندسی

زهره خمر[۱]، فاطمه طباطبایی یزدی[۱*]، سعید زاهدی[۲]

[۱]گروه محیط‌زیست، دانشکده منابع طبیعی و محیط‌زیست، دانشگاه فردوسی مشهد، مشهد، ایران.
[۲]گروه شیلات، دانشکده منابع طبیعی و محیط‌زیست، دانشگاه فردوسی مشهد، مشهد، ایران.

چکیده: این پژوهش به بررسی واکنش‌های ریختی و رشدی بچه‌ماهی‌های کپور معمولی (*Cyprinus carpio*) در برابر چهار فاکتور تنش‌زای محیطی شامل فلز سنگین کادمیوم، آفت‌کش مالاتیون، اسیدیته پایین (pH) و شوری متوسط پرداخته است. تعداد ۱۲۰ نمونه تحت شرایط آزمایشگاهی کنترل‌شده در معرض تیمارها قرار گرفتند. از نمای جانبی چپ نمونه‌ها تصویربرداری استاندارد انجام شد و ۱۸ نقطه نشانه (لندمارک) همولوگ با استفاده از نرم‌افزار tpsDig نشانه‌گذاری گردید. تحلیل‌های ریخت‌سنجی هندسی از جمله برهم‌نهی پروکراست، تحلیل مؤلفه‌های اصلی (PCA)، تحلیل همبستگی کانونی (CVA) و تحلیل تابع تشخیصی (DFA) با بهره‌گیری از نرم‌افزارهای تخصصی انجام شد. نتایج نشان دادند که بین تیمارهای مختلف، تفاوت‌های معنی‌داری در شکل بدن وجود دارد؛ به‌طوری‌که تیمار کادمیوم بیشترین تغییرات ریختی را در نواحی سر و ساقه دمی ایجاد کرد و کاهش معنی‌داری در اندازه مرکزی (centroid size) داشت ($P<۰/۰۰۱$). تیمار pH پایین نیز باعث تغییرات مشخصی در نواحی شکمی و جلویی بدن شد. در مقابل، تیمار شوری منجر به افزایش اندازه مرکزی و بدنی عمیق‌تر گردید که احتمالاً بیانگر واکنش‌های سازشی ریختی برای حفظ تعادل اسمزی است. تیمار مالاتیون نیز اگرچه تغییرات ملایم‌تری ایجاد کرد، اما این تغییرات از نظر آماری معنی‌دار بوده و عمدتاً در نواحی شکمی و سر مشاهده شد. تحلیل‌های CVA و DFA صحت طبقه‌بندی بالایی معادل ۸۱/۳۳ درصد را نشان دادند که بیانگر حساسیت بالای روش ریخت‌سنجی هندسی در شناسایی تغییرات ناشی از تنش‌های محیطی است. این یافته‌ها بر ارزش روش‌های مبتنی بر شکل بدن به‌عنوان شاخص‌های هشدار زودهنگام برای پایش زیست‌محیطی در زیست‌بوم‌های آب شیرین تأکید دارند.

کلمات‌کلیدی: ریخت‌سنجی هندسی، ماهی، انعطاف‌پذیری ریختی، فلزات سنگین، مالاتیون